

<https://doi.org/10.1038/s41526-025-00479-8>

Raman spectroscopy as a tool for assessing plant growth in space and on lunar regolith simulants



Axell Rodriguez¹, Borja Barbero Barcenilla¹, Emily Hall¹, Ishan Kundel¹, Alexander Meyers², Sarah Wyatt³, Dorothy Shippen¹ & Dmitry Kurouski^{1,4}

Colonization of the Moon and other planets is an aspiration of NASA and may yield important benefits for our civilization. The feasibility of such endeavors depends on both innovative engineering concepts and the successful adaptation of life forms that exist on Earth to inhospitable environments. In this study, we investigate the potential of Raman spectroscopy (RS) in a non-invasive and non-destructive assessment of changes in the biochemistry of plants exposed to zero gravity on the International Space Station and during growth on lunar regolith simulants on Earth. We report that RS can sense changes in plant carotenoids, pectin, cellulose, and phenolics, which in turn, could be used to gauge the degree of plant stress in new environments. Our findings also demonstrate that RS can monitor the efficiency of soil supplements that can be used to mitigate nutrient-free regolith media. We conclude that RS can serve as a highly efficient approach for monitoring plant health in exotic environments.

Plants occupy nearly all regions on our planet, including deserts, oceans, and high-altitude regions. They help form ecological niches, produce oxygen and food for animals and humans. They will also be essential components for the successful colonization of the Moon and Mars. During the past decade, substantial effort was made to understand how plant biochemistry changes in such exotic environments^{1,2}. We previously showed that *Arabidopsis thaliana* seedlings cultivated aboard the International Space Station (ISS) exhibited elevated oxidative stress and genome oxidation, yet did not demonstrate a noticeable reduction in telomere length or physiological size¹. We further showed that plants can be successfully cultivated for at least two generations on lunar regolith simulant if the regolith is treated with chemical antioxidants or if plants are genetically modified to express enhanced antioxidant activity². Nevertheless, plants grown on this substrate do not prosper and exhibit reduced biomass and fertility in the next generation, which is accompanied by telomere shortening, decreased telomerase enzyme activity, and increased genome oxidation. These findings indicate that further mitigation efforts will be required to maintain the genome integrity of plants grown in such conditions to enable long-term sustainability².

Confirmatory and quantitative analysis of the biochemical changes associated with growth in these unusual conditions requires sophisticated equipment that cannot be possessed by space shuttles, including the ISS. This problem catalyzed the search for robust and reliable sensors for non-

invasive, non-destructive, and label-free assessment of changes in plant biochemistry induced by many environmental factors. Our group showed that Raman spectroscopy (RS), could be used to meet these strict requirements³. RS is based on the phenomenon of inelastic light scattering^{4,5}. In this case, photons that hit the sample of interest excite the molecules to high vibrational states and scatter back both higher and lower than the incident light. Importantly, the change in the photon energy, which is also known as Raman Shift, directly depends on the chemical structure of molecules present in the sample^{6–8}. Consequently, RS can probe the structure and composition of the sample of interest. Furthermore, because RS is non-invasive and non-destructive, it is ideal for analysis of life systems⁹. During the past decade, several companies have developed hand-held Raman spectrometers that can be used directly in the field or a greenhouse¹⁰.

Expanding upon these advantages of RS, Lee and co-workers investigated the potential of this technique in non-invasive diagnostics of citrus greening disease^{11,12}. It was found that RS could be used to accurately identify citrus greening in both oranges and grapefruits. Furthermore, RS enables specificity by accurate differentiation between the infected plants and nutritionally deficient plants^{11,12}. Recently reported studies employed high-performance liquid chromatography (HPLC) to identify biochemical changes in plants that were sensed by RS¹³. It was found that RS primarily detected changes in lutein and other carotenoids¹³. It was also shown that RS sensed changes in the concentration of small phenolic compounds, such as

¹Department of Biochemistry and Biophysics, Texas A&M University, College Station, TX, USA. ²NASA Postdoctoral Program, Oak Ridge Associated Universities, Kennedy Space Center FL, Merritt Island, FL, USA. ³Molecular and Cellular Biology Program, Ohio University, Athens, OH, USA. ⁴Department of Biomedical Engineering, Texas A&M University, College Station, TX, USA. ✉ e-mail: dshippen@tamu.edu; dkurouski@tamu.edu

coumaric acid, that occurred as a result of plant infection with bacterial, fungal, or viral pathogens¹³. Roy and Prasad recently reported that RS could be used to probe nutritional stress in soybean plants¹⁴, while Yeturu and co-workers demonstrated that RS could be used to diagnose Abutilon mosaic virus in *Abutilon hybridum*¹⁵. Similar findings were recently reported by Juarez and co-workers for diagnosing tomato spotted wilt orthospovirus in tomatoes using a hand-held Raman spectrometer¹⁶.

In the current study, we examine biochemical changes in *A. thaliana* that were grown aboard the ISS. We reasoned that the hand-held nature of RS would be advantageous for on-site measurements compared to classical analytical techniques such as HPLC and HPLC-MS. These traditional methods are laborious and invasive. Furthermore, they generate hazardous waste that would be dangerous in the constrained environment of ISS. A direct comparison of RS to HPLC demonstrated that RS effectively probes changes in the concentration of carotenoids and low molecular weight phenylpropanoids, such as caffeic acid, in plants^{16,17}. Recent results by Juarez

and co-workers confirm that calibration of RS using HPLC overcomes the need for chromatographic techniques for detection and quantification of metal-induced toxicities in plants¹⁷. Therefore, RS holds promise for assessing stress-related plant responses on the ISS. We were also motivated by NASA's beyond Low Earth Orbit colonization plans, and employed RS to examine changes in the biochemistry of plants grown on lunar regolith simulants. Finally, we investigated the extent to which RS could be used to monitor the improvement in the vegetation of regolith-grown plants exposed to antioxidant bio-stimulants such as glutathione, proline, and ascorbic acid.

Results and discussion

Raman spectra acquired from 12-day-old seedlings of Earth-grown *A. thaliana* exhibited vibrational bands that can be assigned to carotenoids, pectin, cellulose and phenylpropanoids, depicted in Fig. 1 and Table 1. We also observed aliphatic vibrations (1326, 1335, and 1440 cm^{-1}), which could

Fig. 1 | Raman spectroscopy reveals striking differences in the biochemistry of *A. thaliana* plants grown on Earth and on the International Space Station (ISS). Averaged Raman spectra (a) acquired from ISS- and Earth-grown *A. thaliana*. Changes in the intensities of vibrational bands that can be assigned to phenylpropanoids (1608 cm^{-1}), carotenoids, (1525 cm^{-1}), pectin (747 cm^{-1}), and cellulose (1048 cm^{-1}) are reported by ANOVA graphs (b). Means of the intensities of vibrational bands are shown by dots; standard deviations by horizontal lines.

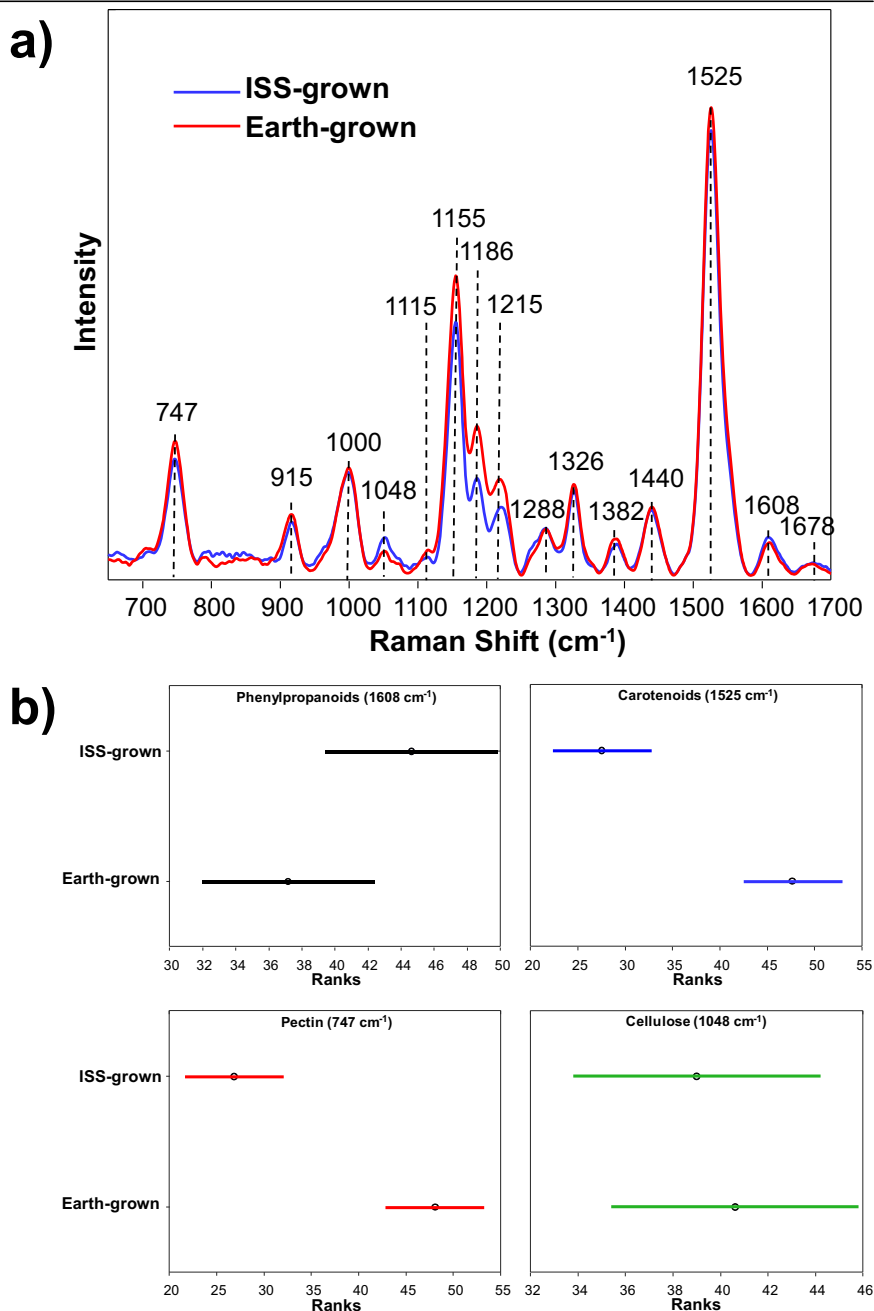


Table 1 | Vibrational band assignments for leaf spectra of *A. thaliana*

Band	Vibrational mode	Assignment
742	$\gamma(\text{C}-\text{O}-\text{H})$ of COOH	Pectin ²⁹
915	$\nu(\text{C}-\text{O}-\text{C})$ In plane, symmetric	Cellulose ¹³ , phenylpropanoids ¹⁷
1000	Aromatics, in-plane CH_3 rocking of polyene	Proteins ³⁰ , carotenoids ^{31,32}
1048	$\nu(\text{C}-\text{O})+\nu(\text{C}-\text{C})+\delta(\text{C}-\text{O}-\text{H})$	Cellulose ¹³ , lignin ³³
1115	$-\text{C}=\text{C}-$	Carotenoids ^{31,32}
1155	$-\text{C}=\text{C}-$	Carotenoids ^{31,32}
1186	$-\text{C}=\text{C}-$	Carotenoids ^{31,32}
1215	$-\text{C}=\text{C}-$	Carotenoids ^{31,32}
1288	$\delta(\text{C}-\text{C}-\text{H})$	Aliphatic, cellulose, phenylpropanoids ^{17,33}
1326	δCH_2 bending	Aliphatic, cellulose, phenylpropanoids ^{17,33}
1335	δCH_2 bending	Aliphatics ²³
1382	δCH_2 bending	Aliphatics ²³
1440	$\delta(\text{CH}_2)+\delta(\text{CH}_3)$	Aliphatics ²³
1525	$-\text{C}=\text{C}-$ (in plane)	Carotenoids ^{31,32}
1608	$\nu(\text{C}-\text{C})$ Aromatic ring+ $\alpha(\text{CH})$	Phenylpropanoids ^{17,34,35}
1678	Amide I	Proteins ³⁰

Table 2 | Confusion matrix of PLS-DA model that indicates the accuracy of identification of Raman spectra acquired from ISS- and Earth-grown plants

	ISS-grown	Earth-grown	Accuracy, %
Predicted as ISS-grown	27	1	90
Predicted as Earth-grown	3	28	96.5

not be assigned to the specific class of compounds due to the presence of these chemical groups in nearly all classes of biological molecules. Raman spectra were also acquired from 12-day-old seedlings of ISS-grown *A. thaliana*, and they had similar vibrational fingerprints. However, we found that the intensity of the phenylpropanoid peak at 1608 cm^{-1} for ISS-grown plants was substantially greater in comparison to the spectra acquired from the leaves of Earth-grown *A. thaliana*. An increase in the intensity of this vibrational band indicates an increase in the concentration of low molecular weight phenylpropanoids. These molecular species are involved in the plant response to biotic and abiotic stresses^{18–20}, arguing that ISS-grown plants experience spaceflight-induced stress that is not observed in Earth-grown plants. This conclusion is further supported by the observed decrease in the intensity of vibrational bands that can be assigned to carotenoids (1115 , 1155 , 1186 , 1215 , and 1525 cm^{-1}). In the case of biotic or abiotic stresses, plants activate the enzymatic degradation of carotenoids, producing abscisic acid^{21,22}. Plant carotenoids can also be oxidised and fragmented by reactive oxygen species (ROS), which results in the formation of β -ionone, β -cyclocitral that activate plant defense mechanisms^{21–23}. These results are in good agreement with the previously reported by Shippen and co-workers of higher ROS activity in ISS-grown plants compared to *A. thaliana* grown on Earth¹.

In the spectra acquired from ISS-grown *A. thaliana* seedlings, we observed an increase in the intensity of the vibrational band centered at 747 cm^{-1} , which can be assigned to pectin. Additionally, we identified small statistically insignificant changes in the intensity of the 1048 cm^{-1} peak, which originates from cellulose. Based on these results, we can conclude that spaceflight alters the structure and composition of pectin, with minimal changes to cellulose, in *A. thaliana*. Additional studies are required to fully understand the chemical nature of changes in these highly important biomolecules in plants.

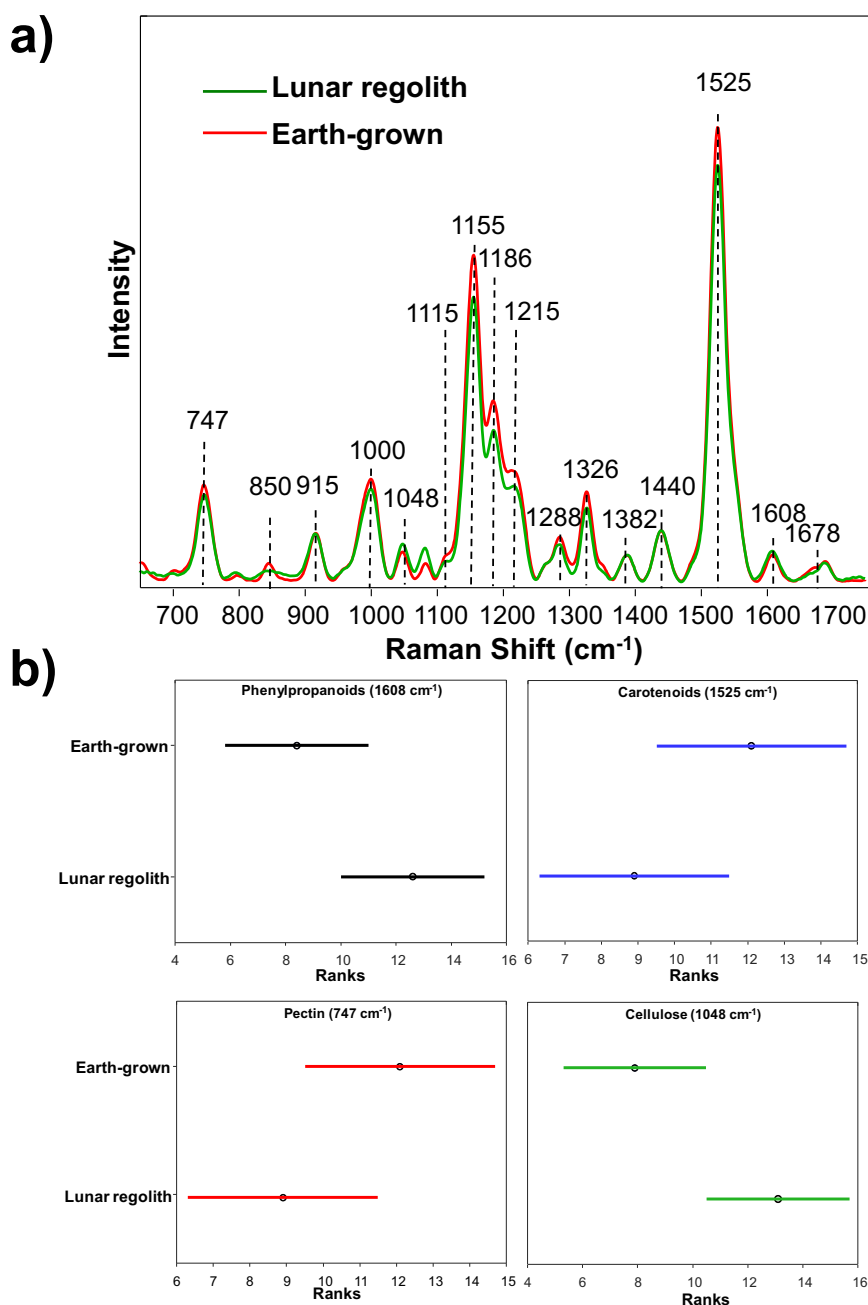
We also performed a partial least-squared discriminant analysis (PLS-DA) to investigate the accuracy of RS-based differentiation between ISS- and Earth-grown *A. thaliana*, Table 2. Previously reported results by our and other research groups demonstrate that PLS-DA performs as well or even better compared to other supervised chemometric algorithms such as support vector machine (SMV), linear discriminant analysis (LDA) or soft independent modeling by class analogy^{5,7,24–26}. Therefore, we utilized this chemometric method for the analysis of our spectroscopic data. Our results showed that PLS-DA enabled 90% accurate identification of ISS- and 96.5% accurate identification of Earth-grown *A. thaliana*. These results demonstrate that RS could be used as a robust and reliable tool to identify gravity-induced stresses in plants.

Next, we investigated the extent to which RS could be used to probe the response of plants grown for 20 days on the lunar regolith simulant LMS–1, media that can be used to mimic the outer crust of the Moon². RS revealed a substantial increase in the intensity of phenylpropanoids and a decrease in the intensity of carotenoids in the Raman spectra acquired from plants grown on lunar regolith simulant compared to plants grown on Earth soil, Fig. 2. Again, these RS findings were consistent with evidence of a stress response for plants grown in lunar regolith simulant². Although no significant changes in the concentration of pectin were detected, we observed statistically significant differences in the intensities of the vibrational band that can be assigned to cellulose (1048 cm^{-1}). Specifically, the intensity of this band was stronger in the spectra acquired from plants grown in the lunar regolith simulant compared to plants grown in conventional Earth soil. These results indicate that regolith-induced stress caused a substantial increase in the synthesis of cellulose, which may help to facilitate the adaptation of *A. thaliana* to this exotic substrate.

We previously showed that the poor or toxic nutritional environment of regolith could be partially overcome by the addition of an antioxidant cocktail composed of 0.75 mM glutathione, 0.75 mM ascorbic acid and 0.75 mM proline, or by its individual components². Expanding upon this, we investigated whether RS could be used to monitor bio stimulant-induced improvement in the plant health, Fig. 3. Based on the changes of the intensities of carotenoids and cellulose vibrations, we found that antioxidant treatment with all three components of the cocktail was the most efficient of all bio stimulants, as depicted on Fig. 3. Specifically, plants grown on the regolith simulant soil treated with antioxidants exhibited comparable intensities of carotenoids and cellulose vibrations to the control plants that were grown in Earth soil. These results demonstrate that antioxidants minimise the enzymatic degradation of plant carotenoids into abscisic acid. High concentration of carotenoids in these plants also suggests that low levels of ROS, which are also known to fragment and degrade carotenoids. Thus, antioxidants minimise the regolith-induced stress of plants. Our results further showed that the individual components of the antioxidant cocktail were able to significantly alter the carotenoid and cellulose RS profiles, Fig. 3. Consistent with these observations, the antioxidant cocktail, as well as individual proline and glutathione treatments, substantially improved plant growth and reduced genome oxidation with respect to untreated lunar regolith².

In addition to LMS–1 Lunar Mare Simulant, other lunar regolith simulants are commercially available that replicate specific lunar environments with high fidelity (Long-Fox et al.)²⁷. These include LHS–1 Lunar Highlands Simulant and LSP–2 Lunar South Pole simulant. We also investigated the extent to which treatment of three different types of lunar regolith with an antioxidant cocktail composed of glutathione, ascorbic acid and proline could change the concentration of phenylpropanoids, carotenoids, pectin and cellulose. For these experiments, we examined more mature plants that were 47 days old. We found that treatment of lunar highlands and lunar mare simulants with the cocktail composed of glutathione, ascorbic acid and proline increased the concentration of phenylpropanoids, carotenoids, and pectin. Interestingly, no substantial changes in the concentration of cellulose were observed, Fig. 4. Such treatment-induced improvements were minor in plants grown on lunar south pole simulants. These findings indicate that the antioxidant-induced increase in the concentration of phenylpropanoids, carotenoids, and pectin in *A. thaliana* depends on the type of simulant that

Fig. 2 | Raman spectroscopy-based assessment of biochemical differences in the plants grown in the Earth soil and lunar regolith simulant (LMS-1). Averaged Raman spectra (a) acquired from Earth- and LMS-1 lunar regolith-grown *A. thaliana*. Changes in the intensities of vibrational bands that can be assigned to phenylpropanoids (1608 cm^{-1}), carotenoids, (1525 cm^{-1}), pectin (747 cm^{-1}), and cellulose (1048 cm^{-1}) are reported by ANOVA graphs (b). Means of the intensities of vibrational bands are shown by dots; standard deviations by horizontal lines.



plants were grown on. Furthermore, compared to 20-day-old LMS-1 grown plants, Fig. 2, 47-day-old LMS-1 plants exhibited reduced levels of carotenoids and pectin relative to the control. The older plants also showed decreased phenylpropanoids and cellulose. These results indicate that secondary metabolite production is dynamic and evolves throughout plant development in lunar regolith simulant.

Taken together, our results indicate that RS is a useful tool for non-invasive and non-destructive assessment of the effect of bio stimulants on the health of plants grown in regolith. Moreover, our RS results are consistent with the results from other biochemical assays and highlight the potential challenges in preserving plant wellbeing in lunar regolith simulant despite efforts at bio-stimulation⁷. Consequently, these results underscore the feasibility of utilizing RS for non-invasive and non-destructive evaluation of the overall health of plants cultivated in regolith.

Summarizing, our findings demonstrate that RS is a useful tool for the confirmatory sensing of changes in plant biochemistry caused by zero gravity and growth in Lunar regolith simulants. Notably, there is an

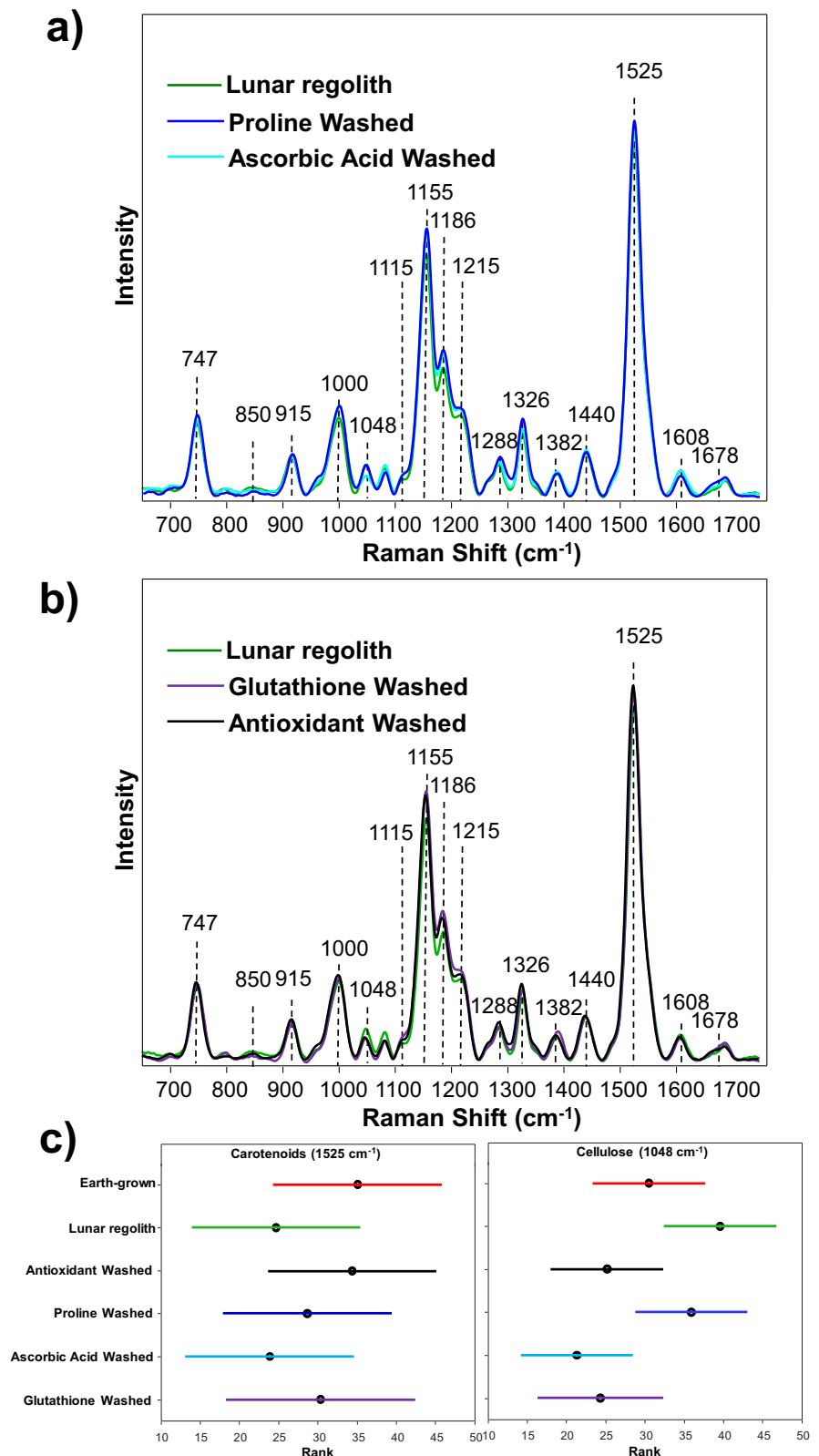
established correlation between carotenoids and phenylpropanoids with stress response and oxidative damage; both plant materials subjected to spaceflight conditions and those cultivated in lunar environments exhibited alterations in the levels of these molecules. The observed changes in carotenoids and phenylpropanoids in space-flown plants and plants grown in simulants of lunar soil suggest a response to stress factors and oxidative challenges experienced in these unique settings. Our results also show that RS could be used to monitor the efficiency of soil supplements that were capable of mitigating the negative effects of nutrient-free regolith media and, consequently, improving the plant health. Thus, RS represents a highly efficient, quick, and label-free approach for monitoring plant health in exotic environments.

Materials and methods

Plant materials

Plant growth. For seedlings grown on the ISS *Arabidopsis thaliana* seeds (35S::HF-RPL18 in the Columbia-0 background; ABRC stock # CS66056)

Fig. 3 | Elucidation of the effect of proline, ascorbic acid, glutathione, and antioxidants on *A. thaliana* grown in lunar regolith simulant (LMS-1). Averaged Raman spectra (a, b) acquired from LMS-1 lunar regolith-grown *A. thaliana*, and regolith washed with proline, ascorbic acid, glutathione, and antioxidants. Changes in the intensities of vibrational bands that can be assigned to carotenoids, (1525 cm^{-1}) and cellulose (1048 cm^{-1}) are reported by ANOVA graphs (c). Means of the intensities of vibrational bands are shown by dots; standard deviations by horizontal lines.



were affixed to a polyethersulfone (PES) membrane using guar gum². Each membrane accommodated fifteen seeds and was subsequently placed onto square 10 cm $0.5\times$ Murashige and Skoog plates with 1% agar. Following a 19-day period of darkness at 4°C , the plates were integrated into the Veggie growth chambers on the ISS and at Kennedy Space Centre, where the plants were cultivated for 12 days under 16 h/8 h long day conditions. The growth

conditions included $100\text{ mol/m}^2/\text{s}$ of red (630 nm), blue (455 nm), and green (530 nm) light, simulating Veggie units. Ground control plates underwent seeding, growth, and harvesting with a 48-hour delay from the flight samples. Environmental conditions such as temperature, CO_2 , and relative humidity were monitored continuously on the ISS and replicated with a 48-hour delay in the ground control environmental chamber. The average temperature

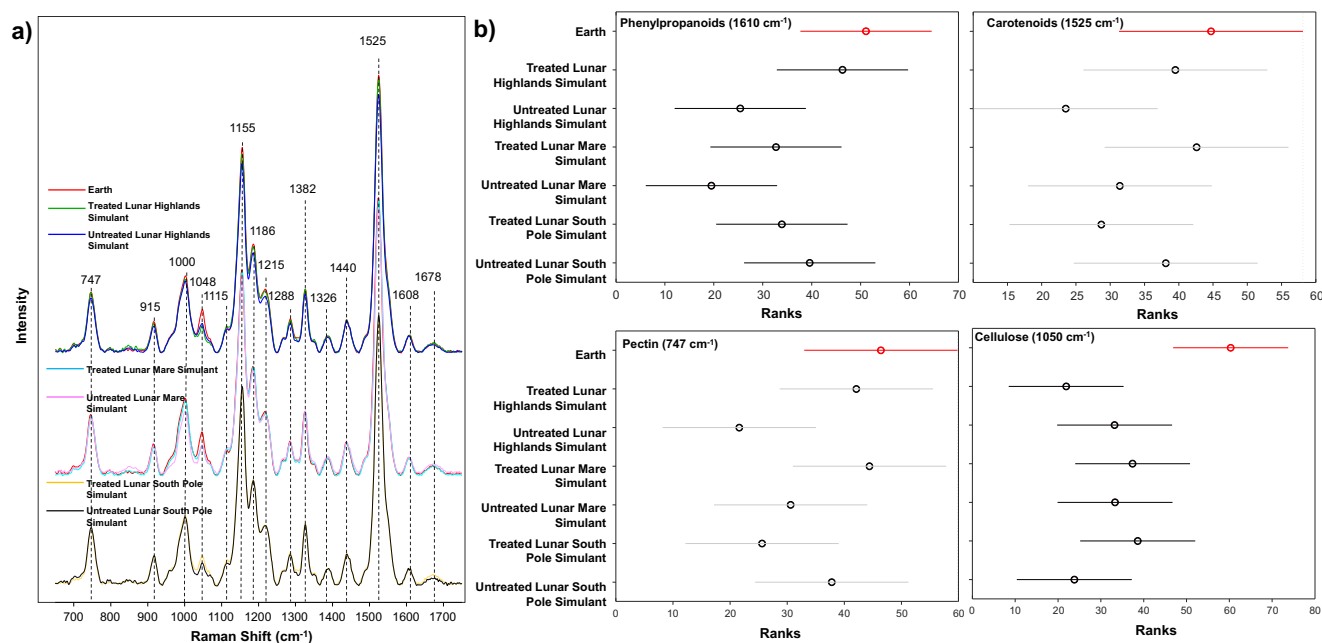


Fig. 4 | Raman spectroscopy monitors biostimulant-induced improvement in the health of *A. thaliana* grown on different soil simulants treated and untreated with bio stimulants. Averaged Raman spectra (a) acquired from *A. thaliana* grown on treated and untreated lunar regolith at 47 days old. Changes in the intensities of vibrational bands that can be assigned to phenylpropanoids (1610 cm^{-1}),

carotenoids, (1525 cm^{-1}), pectin (747 cm^{-1}) and cellulose (1050 cm^{-1}) are reported in the post-hoc graphs for Kruskal–Wallis (b). Mean rank of the intensities of vibrational bands is shown by dots; comparison intervals are shown by horizontal lines.

maintained was $23\text{ }^{\circ}\text{C}$ with 44% relative humidity, and CO_2 levels were typically around 1750 ppm. Following removal from the Veggie, astronauts or ground control staff collected the PES membranes and seedlings using forceps, which were then protected in the lid of the Petri dish, wrapped with foil, and swiftly transferred to a $-130\text{ }^{\circ}\text{C}$ cold bag for rapid freezing. Subsequently, the seedlings were stored at $-80\text{ }^{\circ}\text{C}$, shipped on dry ice, and kept at $-80\text{ }^{\circ}\text{C}$ until processing.

For plant grown on lunar regolith simulant, seeds from Col-0 were procured from The Arabidopsis Biological Resource Centre (ABRC) at Ohio State University, stock CS28994². The seeds underwent surface sterilization in 2.7% sodium hypochlorite for 7 min, followed by stratification at $4\text{ }^{\circ}\text{C}$ for three days. Subsequently, they were directly transferred to their designated treatment of either regolith simulant (LMS-1, LSP-2 and LHS, Exolith Lab, Oviedo, FL, USA) or Earth soil (Sunshine, Mix 5, Sun Gro Horticulture, Agawam, MA, USA). Germination took place under a 12-h photoperiod with an average illuminance of $5000 (\pm 250)$ lux achieved using lights with a 3000:6500 Kelvin ratio, and maintained at a constant temperature of $22\text{ }^{\circ}\text{C}$. The plants were allowed to grow under these conditions for five weeks or until growth ceased, upon which the entire plants were harvested for analysis.

Raman spectroscopy. Raman spectra were collected from the surface of plant leaves with a hand-held Resolve Agilent spectrometer equipped with an 830-nm laser source. Spectral resolution was 15 cm^{-1} . The following experimental parameters were used for all collected spectra: 1 s integration time, 495 mW power, and baseline spectral subtraction by device software. Absence of photodegradation under these experimental conditions was previously demonstrated by our group¹². Thirty spectra were collected from leaves of each group of plants. The laser post on the surface was $\sim 2\text{ mm}$ in diameter. Spectra shown in the manuscript are processed through MATLAB, normalizing on 1440 cm^{-1} peak, which corresponds to CH_2 vibration, which is present in nearly all classes of biological molecules, and applied with Savitzky-Golay smoothing using a polynomial order of 0.

Machine learning model. In this work, we utilized PLS-DA and analysis of variance (ANOVA) using MATLAB equipped with PLS_Toolbox 9.0 (Eigenvector Research Inc., Manson, WA). This supervised version of PLS achieves dimensionality reduction by transforming classified data into sets of latent variables (LVs), each designed to maximize covariance between the dataset and the classes. The number of LVs used for each model was selected to maximize model accuracy while minimizing model bias. A total of five LVs were used for each PLS-DA model: LV 1 (39.14%), LV 2 (25.51%), LV 3 (2.96%), LV 4 (2.01%), and LV 5 (1.84%), totaling 71.46%. Each LV percentage depicts the covariance of the predictor and response variables (X, Y), which are associated with building the model. A Kruskal–Wallis test is paired with a multcompare statistical function to determine the differences between specific groups and their significance²⁸.

Data availability

The data that support the findings of this study are available upon request from the corresponding author [D.K.].

Received: 25 July 2024; Accepted: 17 May 2025;

Published online: 27 May 2025

References

1. Barcenilla, B. B. et al. Arabidopsis telomerase takes off by uncoupling enzyme activity from telomere length maintenance in space. *Nat. Commun.* **14**, 7854 (2023).
2. Barcenilla, B. B. et al. Telomere dynamics and oxidative stress in Arabidopsis grown in lunar regolith simulant. *Front. Plant Sci.* **15**, 1351613 (2024).
3. Farber, C., Wang, R., Chemelewski, R., Mullet, J. & Kourouski, D. Nanoscale structural organization of plant epicuticular wax probed by atomic force microscope infrared spectroscopy. *Anal. Chem.* **91**, 2472–2479 (2019).
4. Payne, W. Z. & Kourouski, D. Raman-based diagnostics of biotic and abiotic stresses in plants. A review. *Front. Plant Sci.* **11**, 616672 (2021).

5. Gupta, S. et al. Portable Raman leaf-clip sensor for rapid detection of plant stress. *Sci. Rep.* **10**, 20206 (2020).
6. Krimmer, M., Farber, C. & Kurouski, D. Rapid and noninvasive typing and assessment of nutrient content of maize kernels using a Handheld Raman spectrometer. *ACS Omega* **4**, 16330–16335 (2019).
7. Mandrile, L. et al. Nondestructive Raman spectroscopy as a tool for early detection and discrimination of the infection of tomato plants by two economically important viruses. *Anal. Chem.* **91**, 9025–9031 (2019).
8. Sanchez, L., Pant, S., Mandadi, K. & Kurouski, D. Raman spectroscopy vs quantitative polymerase chain reaction in early stage huanglongbing diagnostics. *Sci. Rep.* **10**, 10101 (2020).
9. Farber, C., Mahnke, M., Sanchez, L. & Kurouski, D. Advanced spectroscopic techniques for plant disease diagnostics. a review. *Trends Anal. Chem.* **118**, 43–49 (2019).
10. Juarez, I. D. & Kurouski, D. Contemporary applications of vibrational spectroscopy in plant stresses and phenotyping. *Front. Plant Sci.* **15**, 1411859 (2024).
11. Sanchez, L., Pant, S., Irey, M. S., Mandadi, K. & Kurouski, D. Detection and identification of canker and blight on orange trees using a hand-held Raman spectrometer. *J. Raman Spectrosc.* **50**, 1875–1880 (2019).
12. Sanchez, L., Pant, S., Xing, Z., Mandadi, K. & Kurouski, D. Rapid and noninvasive diagnostics of Huanglongbing and nutrient deficits on citrus trees with a handheld Raman spectrometer. *Anal. Bioanal. Chem.* **411**, 3125–3133 (2019).
13. Dou, T. et al. Biochemical origin of raman-based diagnostics of huanglongbing in grapefruit trees. *Front. Plant Sci.* **12**, 680991 (2021).
14. Roy, M. & Prasad, A. Raman spectroscopy for nutritional stress detection in plant vascular tissue. *Materialia* **24**, 101474 (2022).
15. Yeturu, S. et al. Handheld Raman spectroscopy for the early detection of plant diseases: abutilon mosaic virus infecting Abutilon sp. *Anal. Methods* **8**, 3450–3457 (2016).
16. Juarez, I. D. et al. Using Raman spectroscopy for early detection of resistance-breaking strains of tomato spotted wilt orthospovirus in tomatoes. *Front. Plant Sci.* **14**, 1283399 (2023).
17. Juarez, I. D., Dou, T., Biswas, S., Septiningsih, E. M. & Kurouski, D. Diagnosing arsenic-mediated biochemical responses in rice cultivars using Raman spectroscopy. *Front. Plant Sci.* **15**, 1371748 (2024).
18. Deng, Y. & Lu, S. Biosynthesis and regulation of phenylpropanoids in plants. *Crit. Rev. Plant Sci.* **36**, 257–290 (2017).
19. Cheynier, V., Comte, G., Davies, K. M., Lattanzio, V. & Martens, S. Plant phenolics: Recent advances on their biosynthesis, genetics, and ecophysiology. *Plant Physiol. Biochem.* **72**, 1–20 (2013).
20. Sharma, A. et al. Response of phenylpropanoid pathway and the role of polyphenols in plants under abiotic stress. *Molecules* **24**, 2452 (2019).
21. Havaux, M. Carotenoid oxidation products as stress signals in plants. *Plant. J.* **79**, 597–606 (2013).
22. Nambara, E. & Marion-Poll, A. Absciscic acid biosynthesis and catabolism. *Annu. Rev. Plant Biol.* **56**, 165–185 (2005).
23. Yu, M. M., Schulze, H. G., Jetter, R., Blades, M. W. & Turner, R. F. Raman microspectroscopic analysis of triterpenoids found in plant cuticles. *Appl. Spectrosc.* **61**, 32–37 (2007).
24. Farber, C. et al. Raman-based diagnostics of stalk rot disease of maize caused by *Colletotrichum graminicola*. *Front. Plant Sci.* **12**, 722898 (2021).
25. Farber, C. et al. Potential of spatially offset raman spectroscopy for detection of zebra chip and potato virus y diseases of potatoes (*Solanum tuberosum*). *ACS Agric. Sci. Technol.* **1**, 211–221 (2021).
26. Farber, C., Shires, M., Ong, K., Byrne, D. & Kurouski, D. Raman spectroscopy as an early detection tool for rose rosette infection. *Planta* **250**, 1247–1254 (2019).
27. Long-Fox, J. M. & Britt, D. T. Characterization of planetary regolith simulants for the research and development of space resource technologies. *Front. Space Technol.* **4**, <https://doi.org/10.3389/frspt.2023.1255535> (2023).
28. Joshi, R. et al. Raman spectral analysis for non-invasive detection of external and internal parameters of fake eggs. *Sens. Actuators B: Chem.* **303**, 127243 (2020).
29. Synytsya, A., Čopíková, J., Matějka, P. & Machovič, V. Fourier transform Raman and infrared spectroscopy of pectins. *Carbohydr. Polym.* **54**, 97–106 (2003).
30. Kurouski, D., Van Duyne, R. P. & Lednev, I. K. Exploring the structure and formation mechanism of amyloid fibrils by Raman spectroscopy: a review. *Analyst* **140**, 4967–4980 (2015).
31. Devitt, G., Howard, K., Mudher, A. & Mahajan, S. Raman spectroscopy: an emerging tool in neurodegenerative disease research and diagnosis. *ACS Chem. Neurosci.* **9**, 404–420 (2018).
32. Adar, F. Carotenoids - their resonance Raman spectra and how they can be helpful in characterizing a number of biological systems. *Spectroscopy* **32**, 12–20 (2017).
33. Edwards, H. G., Farwell, D. W. & Webster, D. FT Raman microscopy of untreated natural plant fibres. *Spectrochim. Acta A* **53**, 2383–2392 (1997).
34. Kang, L., Wang, K., Li, X. & Zou, B. High pressure structural investigation of benzoic acid: Raman spectroscopy and x-ray diffraction. *J. Phys. Chem. C* **120**, 14758–14766 (2016).
35. Agarwal, U. P. Raman imaging to investigate ultrastructure and composition of plant cell walls: distribution of lignin and cellulose in black spruce wood (*Picea mariana*). *Planta* **224**, 1141–1153 (2006).

Acknowledgements

This study was supported by funds from Texas A&M AgriLife Research, Texas A&M University Governor's University Research Initiative (GURI) grant program of (12-2016/M1700437), by the National Institutes of Health (R01 GM065383 to D.E.S.), the National Aeronautics and Space Administration (80NSSC19K1481 to S.E.W.; 80NSSC23K0302 to D.E.S and S.E.W.) and the NASA Postdoctoral Program at Kennedy Space Center administered by Oak Ridge Associated Universities (to A.M.). We extend our gratitude to the APEX-07 team, with special acknowledgement to Gerard Newsham, Anne Marie Campbell, Erica Bugarner, and Susan Manning-Roach, based at Kennedy Space Center, for their dedication to experiment validation, flight preparation, and return. We also express our appreciation to astronauts Thomas Pesquet, Mark Vande Hei, and Megan McArthur for their assistance with experiment takedown and harvest on the ISS.

Author contributions

A.R. performed Raman measurements and chemometric analyses of data, interpreted and visualized results; wrote and edited the manuscript; B.B.B. performed plant experiments, wrote, and edited the manuscript; E.H. performed plant experiments; I.K. performed plant experiments; A.M. prepared plant material for spaceflight experiments; S.W. supervised spaceflight experiments; D.S. conceptualized the work, supervised study, wrote and edited the manuscript; D.K. supervised study, interpreted and visualized results; wrote and edited the manuscript.

Competing interests

The authors declare no competing interests.

Additional information

Correspondence and requests for materials should be addressed to Dorothy Shippen or Dmitry Kurouski.

Reprints and permissions information is available at <http://www.nature.com/reprints>

Publisher's note Springer Nature remains neutral with regard to jurisdictional claims in published maps and institutional affiliations.

Open Access This article is licensed under a Creative Commons Attribution-NonCommercial-NoDerivatives 4.0 International License, which permits any non-commercial use, sharing, distribution and reproduction in any medium or format, as long as you give appropriate credit to the original author(s) and the source, provide a link to the Creative Commons licence, and indicate if you modified the licensed material. You do not have permission under this licence to share adapted material derived from this article or parts of it. The images or other third party material in this article are included in the article's Creative Commons licence, unless indicated otherwise in a credit line to the material. If material is not included in the article's Creative Commons licence and your intended use is not permitted by statutory regulation or exceeds the permitted use, you will need to obtain permission directly from the copyright holder. To view a copy of this licence, visit <http://creativecommons.org/licenses/by-nc-nd/4.0/>.

© The Author(s) 2025